

Metallomics

Accepted Manuscript



This is an *Accepted Manuscript*, which has been through the Royal Society of Chemistry peer review process and has been accepted for publication.

Accepted Manuscripts are published online shortly after acceptance, before technical editing, formatting and proof reading. Using this free service, authors can make their results available to the community, in citable form, before we publish the edited article. We will replace this *Accepted Manuscript* with the edited and formatted *Advance Article* as soon as it is available.

You can find more information about *Accepted Manuscripts* in the [Information for Authors](#).

Please note that technical editing may introduce minor changes to the text and/or graphics, which may alter content. The journal's standard [Terms & Conditions](#) and the [Ethical guidelines](#) still apply. In no event shall the Royal Society of Chemistry be held responsible for any errors or omissions in this *Accepted Manuscript* or any consequences arising from the use of any information it contains.

1
2
3 **1 Cu binding by the *Escherichia coli* metal-efflux accessory protein RcnB**

4
5
6 2
7 3 Camille Blériot ^{1,5 §}, Manon Gault ^{1 §}, Erwan Gueguen ¹, Pascal Arnoux ^{2,3,4}, David
8 4 Pignol ^{2,3,4}, Marie-Andrée Mandrand-Berthelot ¹ and Agnès Rodrigue ^{1*}

9
10
11
12
13
14 5
15 6
16 7
17 8 ¹ Microbiologie, Adaptation et Pathogénie, UMR5240 CNRS INSA Lyon Université
18 9 Lyon 1, F-69621 Villeurbanne, France.

19 10 ² CEA, DSV, IBEB, Lab Bioenerget Cellulaire, Saint-Paul-lez-Durance, F-13108,
20 11 France.

21 12 ³ CNRS, UMR Biol Veget & Microbiol Environ, Saint-Paul-lez-Durance, F-13108,
22 13 France.

23 14 ⁴ Aix-Marseille Université, Saint-Paul-lez-Durance, F-13108, France.

24 15 ⁵ Present address : Institut Pasteur, Inserm U1117, 75724 Paris Cedex 15 France

25 16 [§] contributed equally to this work

26
27
28
29
30
31
32
33
34
35
36
37 19 * For correspondence:

38 20 Agnès Rodrigue

39 21 MAP UMR 5240 CNRS- INSA Lyon-UCBL

40 22 Bat Lwoff – 10 rue Dubois

41 23 F- 69622 Villeurbanne Cedex

42 24 Phone : (+33) 472447980 - Fax : (+33) 472431584

43 25 e-mail : agnes.rodrigue@insa-lyon.fr

44
45
46
47
48
49
50
51
52
53
54
55
56
57
58
59
60

1
2
3 28 **Abstract**

4 29 Divalent cations play fundamental roles in biological systems where they act as
5 30 structural and reactive determinants. Their high reactivity with biomolecules have forced
6 31 living cells to evolve specific pathways for their *in vivo* handling. For instance the excess of
7 32 metal can be expelled by dedicated efflux systems. The *E. coli* RcnA efflux pump expels both
8 33 Ni and Co. This pump functions together with the periplasmic protein RcnB to maintain metal
9 34 ion homeostasis. To gain insights into the efflux mechanism, metal binding properties of
10 35 RcnB were investigated. Initial screening of metal ions by fluorescence quenching elicited Cu
11 36 as a potential ligand for RcnB. Non-denaturing mass spectrometry and ITC experiments
12 37 revealed the binding of one Cu ion per monomer with a micromolar affinity. This set of *in*
13 38 *vitro* techniques was broadened by *in vivo* experiments that showed the accuracy of Cu
14 39 binding by RcnB. RcnB implication in Cu detoxification was questioned and growth
15 40 experiments as well as transcriptional analysis excluded a role for RcnB in Cu adaptation.
16 41 Finally a mutant in a conserved Methionine residue (Met86) displayed altered Cu binding.
17 42 This mutant protein when tested for its Ni and Co resistance capacity was unable to
18 43 complement an *rcn* mutant. Taken together these data show that RcnB is a new Cu-binding
19 44 protein that is strikingly involved in a Ni/Co efflux system.
20
21
22
23
24
25
26
27
28
29
30
31
32
33
34
35
36
37
38
39
40
41
42
43
44
45

1
2
3 464 47 **Introduction**

5 48 Metal ions are essential components of all living cells including bacteria. Among
6 49 metals, cobalt (Co), either as a co-factor or associated with vitamin B12, is required for many
7 50 biological functions¹. Nickel (Ni) is a catalytic cofactor of several prokaryotic enzymes, the
8 51 best characterized being hydrogenases and ureases². Copper (Cu) is mainly involved in redox
9 52 reactions permitting, by cycling between the cupric Cu(II) and cuprous Cu(I) forms, to
10 53 oxidize a wide variety of substrates³.

11 54 However, like many other transition metals, Ni, Co or Cu are toxic when present in
12 55 excess, causing growth arrest and cell death. Toxicity can result from the non specific
13 56 interactions between metal ions and proteins or DNA⁴. Another mechanism of toxicity is the
14 57 oxidative stress, which can lead to the creation of hazardous reactive oxygen species⁵⁻⁶.
15 58 Furthermore, an excess of Co impairs the biogenesis of Fe/S clusters by a direct competition
16 59 with iron⁷.

17 60 The most widespread mechanism bacteria use to overcome this toxicity is the efflux of
18 61 these cations out of cells. Ni and Co are often expelled by the same efflux pumps. In
19 62 *Escherichia coli*, the RcnA efflux pump is the only known system responsible for the
20 63 cytoplasmic detoxification of Ni and Co. RcnA is an inner membrane protein, widespread in
21 64 bacteria, thought to function as a secondary transporter⁸. The expression of *rcnA* is
22 65 specifically induced *in vivo* by Ni and Co and not by other divalent cations as shown by using
23 66 reporter gene fusion^{8,9}.

24 67 The metallo-regulator RcnR represses the expression of *rcnA*⁹ as well as its own
25 68 expression through binding on the shared operator site of these two divergently transcribed
26 69 genes¹⁰. *In vitro*, Ni and Co are able to dissociate RcnR from its cognate DNA binding site
27 70 whereas Zn or Cu display the same effect for concentrations 4 to 8 times higher respectively
28 71¹⁰. RcnR, like most of the metallo-regulators, is involved in maintaining metal homeostasis by
29 72 controlling the expression of the metal transporter. We have shown recently that a second
30 73 protein, RcnB, is essential to control Ni and Co intracellular levels in *E. coli*¹¹. In contrast to
31 74 RcnR, RcnB is periplasmic and its mode of action which is actually unclear, does not seem to
32 75 reside in a regulatory event¹¹. Still RcnB is thought to act as a modulator of the efflux
33 76 mediated by the RcnA pump and is required to maintain proper metal homeostasis¹¹.

34 77 In this work, in the course of identifying ligands for RcnB, we detected Cu as being a
35 78 co-factor of RcnB. Cu-binding proteins described so far are either involved in redox reactions,
36 79 in maintaining Cu homeostasis, or act as chaperones¹². As Cu can undergo redox cycling
37 80

1
2
3 80 between Cu(I) and Cu(II) oxidation states, it can act as an electron acceptor/ donor like in
4 81 cytochrome oxidase or is present in redox active enzymes like superoxide dismutase. It is
5 82 noteworthy that all bacterial Cu-requiring enzymes are extracytoplasmic, with the exception
6 83 of cyanobacteria that contain Cu-enzymes within internal membrane-bound compartments³.
7
8 84 Cu is highly toxic in the cytoplasm¹³ and cells require systems to overcome this danger. In *E.*
9 85 *coli* the inner membrane P-type ATPase CopA constitutes the core element of Cu resistance.
10 86 *copA* is inducible by Cu in both anaerobic and aerobic conditions¹⁴. A second resistance
11 87 system is the periplasmic multi-Cu oxidase CueO that oxidizes Cu(I) ions in less toxic Cu(II)
12 88 ions¹⁵. Since the enzyme activity is dependent on oxygen CueO works strictly under aerobic
13 89 conditions. Briefly, CueO contains Cu active sites that can oxidize several substrates, one of
14 90 them being Cu(I) ions¹⁶. The last system, Cus, is composed of a RND-driven tripartite efflux
15 91 complex, CusCBA, and a soluble periplasmic Cu-binding protein, CusF¹⁷. The molecular
16 92 mechanism is not fully understood yet but it is thought to correspond to a switch model where
17 93 Cu primary binds to CusF that transfers it to CusB. This step induces a conformational change
18 94 that allows periplasmic Cu ions to be taken in charge by CusA and expelled via CusC¹⁸. The
19 95 Cus system is predominantly active under anaerobic conditions and a mutant strain has been
20 96 shown to be Cu sensitive¹⁹.

21 97 Here we show that RcnB, which does not bind Ni and Co ions directly¹¹, is able to
22 98 bind copper. Using a combination of biophysical methods, the *in vitro* binding properties of
23 99 Cu by RcnB were characterized. This binding was further investigated and shown to occur *in*
24 100 *vivo*. As RcnB is a periplasmic protein, its implication in Cu homeostasis was assessed.
25 101 Physiological experiments clearly demonstrated that RcnB is not a partner of systems
26 102 controlling cellular Cu level and that RcnB plays no role in Cu tolerance. Finally the use of
27 103 copper as a co-factor for RcnB activity was examined. Mutagenesis of the motif
28 104 (H₈₂W₈₃XXM₈₆) conserved among RcnB homologs was carried out. Interestingly, mutant
29 105 M86A RcnB showed altered Cu-binding and lost the ability to control Ni and Co homeostasis.
30 106 As a conclusion, RcnB is a novel copper-binding protein and copper is essential for the
31 107 activity of RcnB.

32 108

33 109 **Materials and Methods**

34 110 **Bacterial strains, plasmids and culture conditions**

35 111 Strains and plasmids used in this work are summarized in Table 1 and are all
36 112 derivatives of *E. coli* K-12. Bacterial cells were grown in LB medium and cultures were
37 113 performed at 37°C unless otherwise stated. Anaerobic conditions were obtained by placing

1
2
3 114 Petri dishes in a GasPak jar, according to the manufacturer's instructions (BD). Where
4
5 115 required, antibiotics purchased from Sigma were used at the following concentrations:
6
7 116 chloramphenicol (Cam) at 20 µg/mL, kanamycin (Kan) at 50 µg/mL, ampicillin (Amp) at 100
8
9 117 µg/mL. *cusF*, *copA* and *cueO* mutant strains were obtained from the KEIO collection ²⁰.
10
11 118 Mutant genes were further transferred from strain BW25113 to strain W3110 or WRCB1, via
12
13 119 generalized phage transduction using P1 vir, as described by Miller ²¹. The $\Delta rcnA\Delta rcnB$
14
15 120 mutant was constructed by deletion of the corresponding genes. For that purpose, a 0.5-kb
16
17 121 fragment corresponding to the immediately upstream region of *rcnA* was amplified using
18
19 122 oligos pair L28 (CGGCCGCGGACCGGATGCGATGATAAATCGCAGAG) and L29
20
21 123 (GCTTTTTTTAGCGATGTTTCGGTCATGATAATAATTCTTAG). A 0.5-kb fragment
22
23 124 corresponding to the immediately downstream region of *rcnB* was amplified using oligos pair
24
25 125 L30 (TATTATCATGACCGAACATCGCTAAAAAAGCCCCCTC) and L31
26
27 126 (GGCCGCTCTAGAGGACAGCCACAGGTAACAAAGCA). Both PCR-amplified DNA
28
29 127 fragments were directly cloned into *Bam*HI-linearized gene replacement pKO3 vector ²²,
30
31 128 using the SLIC cloning method ²³. The *E. coli* W3110 $\Delta rcnAB$ in-frame deletion mutant was
32
33 129 then constructed following the method described previously ²². Site directed mutagenesis of
34
35 130 *rcnB* was performed using the QuikChange site-directed mutagenesis kit according to the
36
37 131 manufacturer's instructions (Stratagene). The sequence of the plasmid was verified
38
39 132 subsequently.
40
41 133

134 **Ni and Cu susceptibility testing**

135 Plate assay metal-sensitivity assays were conducted as follows: first, bacteria were
136
137 grown until mid-log phase in LB medium. A 10-fold serial dilution of the cultures in M63
138
139 medium was performed and 5 µL were spotted onto 0.4% glucose M63 minimal medium
140
141 plates containing increasing concentrations of metal. The plates were incubated at 37°C for
142
143 24-48 h, under aerobic conditions, or for 48-72 h under anaerobic conditions. Susceptibility
144
145 testing in liquid cultures was conducted in M63 medium supplemented with 0.4% glucose.
146
147 Cultures were incubated at 37°C for 16h and the number of bacteria estimated using OD_{600nm}.
148
149 The RcnAB efflux system was previously shown to be specific for Ni or Co ^{8,11}, in this study
150
151 Ni was employed as the cognate metal of the system. As the *in vitro* experiments performed
152
153 here demonstrated an interaction between RcnB and Cu, exposition to this metal was also
154
155 tested at the physiological level.

156 **Overexpression and purification of the RcnB protein**

1
2
3 147 Overexpression and purification of RcnB were performed as previously described ¹¹.
4
5 148 The purification process is illustrated on supplementary Figure 1. Strain BL21, harboring the
6
7 149 pETRCB plasmid, was grown to mid-log phase in LB medium. Next, 1 mM isopropyl β -D
8
9 150 thiogalactopyranoside (IPTG) was added to induce the expression of RcnB. After 4 h at 30°C,
10
11 151 cells were harvested by centrifugation and either frozen at -80°C for later use or diluted in 50
12
13 152 mM Tris-HCl, pH 7, supplemented with 1.5 M ammonium sulfate and lysed by 3 passages
14
15 153 through a French press in the presence of Halt protease inhibitor (Thermo). The supernatant
16
17 154 was filtered through a 0.45 μ m filter and loaded onto a phenyl HP column (HiTrap, GE
18
19 155 Healthcare). Elution followed a linear gradient, from 1.5 M to 0 M ammonium sulfate in 50
20
21 156 mM Tris-HCl, pH 7, and fractions containing the RcnB protein (0.7 M ammonium sulfate)
22
23 157 were pooled and dialyzed against 50 mM Tris-HCl, pH 7 to remove the ammonium sulfate.
24
25 158 The fraction containing RcnB was then loaded onto an anion-exchange UnoQ1 column (Bio-
26
27 159 Rad). Under these conditions, RcnB was not retained on the column, in contrast to the
28
29 160 contaminating proteins present in the loaded fraction. The purity of RcnB was verified on a
30
31 161 15% Tris-Tricine polyacrylamide gel. When necessary, purified RcnB was concentrated using
32
33 162 6-kDa cut-off Vivaspin 6 concentrators (Sartorius). RcnB was quantified either by measuring
34
35 163 OD_{278nm} using an ϵ of 21430 M⁻¹cm⁻¹ or using the Bradford protein assay kit (Bio-Rad).
36
37 164 Typically, the purification process yielded 20 mg of pure RcnB per liter of culture.

33 165 **Circular dichroism Spectroscopic Analysis**

34
35 166 RcnB protein was used at a final concentration of 25 μ M in 50 mM sodium phosphate
36
37 167 buffer (pH 7.0). Spectra were recorded on a spectrometer Chirascan (Applied Photophysics
38
39 168 Ltd) between 195 and 260 nm. Ni²⁺ and Cu²⁺ ions were added at the same concentration of 25
40
41 169 μ M and incubated 5 minutes at 25°C before the analysis. Denaturation was performed by
42
43 170 increasing gradually (1°C.min⁻¹) the temperature to 90°C and circular dichroism at 220 nm
44
45 171 was monitored in order to follow the unfolding process. Then, renaturation was accomplished
46
47 172 by decreasing the temperature to 25°C (10°C.min⁻¹). Algorithmic deconvolution was
48
49 173 performed by using methods SELCON3, CONTIN, CDSSTR and K2D available on the on-
50
51 174 line server Dichroweb (dichroweb.cryst.bbk.ac.uk) ²⁴.

50 175 **Fluorescence spectroscopy**

51
52 176 Fluorescence quenching of RcnB protein was monitored between 300 and 400 nm
53
54 177 with an excitation wavelength of 280 nm. Protein was dissolved in 100 mM Bis-Tris propane
55
56 178 buffer (pH 6.0) to a final concentration of 5 μ M. At each step, a ten-fold excess of metal ions
57
58 179 solution was titrated into the protein solution with a volume variation below 1 % and
59
60

180 incubated for 5 min at room temperature before the analysis. Cu(II) ions were given by a
181 solution of CuSO₄.

182 Isothermal Titration Calorimetry (ITC)

183 ITC measurements were performed on a Microcal (Northampton, MA) ITC200
184 microcalorimeter at 30 °C in 10 mM Pipes buffer (pH 7.0). For a titration experiment,
185 approximately 250 μL of protein (150 μM) was placed in a reaction cell and injected with the
186 Cu(II) solution (1.5 mM). The first injection was 2 μL, and all subsequent injections were 4
187 μL. A total of 14 injections were made with 2 min intervals between each injection. To ensure
188 adequate mixing, the reaction cell was continuously stirred at 1000 rpm. The heat due to
189 dilution, mechanical effects, and other nonspecific effects was identified by averaging the last
190 three points of the titration and subtracting that value from all data points. The enthalpy
191 changes observed in the control titrations of Cu(II) into buffer and of buffer into apo-RcnB
192 were not significant (data not shown) but were subtracted to obtain the results shown on the
193 Fig. 1C. A single-site binding model was used to fit the data using the ORIGIN software
194 (Microcal). The software uses a nonlinear least-squares algorithm and the concentrations of
195 the species to fit the enthalpy change per injection to an equilibrium binding equation. The
196 binding enthalpy change (ΔH), association constant (K_a), and binding stoichiometry (n) were
197 permitted to float during the least-squares minimization process and taken as the best-fit
198 values.

199 Mass spectrometry

200 5 μM of apo-RcnB were reconstituted with or without a ten-fold excess of Cu²⁺ ions in 20
201 mM ammonium acetate buffer (pH 7.0). The mass measurements were performed in a
202 positive ion mode using ESI-Q-TOF. All the parameters were systematically optimized in
203 denaturing conditions in the presence of 0.2 % formic acid. Data acquisition and analysis
204 were performed using the instrument's Analyst software.

205 RT-PCR assays

206 Total RNA was isolated from liquid cultures of WT *E. coli* cells with the RNeasy kit (Qiagen)
207 and treated twice with DNase (Ambion) for 30 min at 37°C. The absence of DNA
208 contamination was verified by direct PCR. RNA was quantified by measuring the optical
209 density at 260 nm, and its integrity was confirmed by agarose gel electrophoresis. RNA was
210 reverse transcribed using the Access RT-PCR kit (Promega). The following primers were
211 used: YohN1RQ (CACCGTCGTAGGCTTTAATG) and YohN2FQ
212 (GGCAGGAAAGATATGCGACT); YoNup
213 (CTTCAGCCCCATATGATTCTTAAATCAGC) and Yodwn2

1
2
3 214 (CCACCATATAGGTCCAG) ; CusFup (TGACTTTTAACTCCAGGAGAG) and CusFdwn
4 215 (TTTTCATCTCATTAAACCTGGG); and CueOup (GTTTGATTTTGTTCGCCTGC) and
5 216 CueOdwn (CGGGCATATTTCCGAATACG) for the amplification of the *rcnB_{int}*, *rcnB_{ext}*,
6 217 *cusF* and *cueO* transcripts, respectively. Controls were treated as samples, but reverse
7
8 218 transcriptase (RT) was omitted. PCR and RT-PCR products were visualized on a 2% agarose
9
10 219 gel.

220 UV-Visible spectroscopy

14 221 UV-visible (UV-vis) absorption spectra were obtained at 25°C on a Nicolet Evolution 100
15 222 spectrophotometer. Purified apo-RcnB was diluted in 50 mM Tris-HCl, pH 7.0 buffer at a
16 223 final concentration of 130 μM. Equivalents of Cu(II) (donor solution : CuSO₄) were added
17 224 with a volume variation below 1 % step by step and absorption spectra were recorded from
18 225 350 to 850 nm after 5 minutes of equilibration.
19
20
21
22
23
24
25

226 227 228 Results

229 230 RcnB is a Cu-binding protein

31 231 RcnB was previously shown to be essential to control Ni and Co homeostasis¹¹. Some
32 232 direct and indirect experiments were performed but failed to show interactions between
33 233 purified RcnB and Ni or Co ions. RcnB possesses two tryptophan residues in its mature form
34 234 and can generate a strong fluorescence emission signal after an excitation at $\lambda = 280$ nm (Fig.
35 235 1A). This signal was not altered upon addition of 100 μM (i.e. 20 metal equivalents) Ni and
36 236 Co ions or other divalent cations like Zn or Mg (data not shown). In contrast, addition of
37 237 increasing amounts of Cu ions quenched gradually this signal showing that this metal altered
38 238 the environment of at least one tryptophan residue (Fig. 1A). These results suggest that Cu is
39 239 a ligand of RcnB, at least *in vitro*. However, the binding isotherm indicated saturation for 10
40 240 equivalents of Cu or more. This could reflect a global weak affinity of RcnB for Cu or this
41 241 could be due to the presence of several binding sites, some having a weak affinity for Cu.
42
43
44
45
46
47
48

49 242 To characterize the *in vitro* metal-protein stoichiometry, mass spectroscopy was used.
50 243 RcnB was incubated or not with a ten-fold excess of Cu(II) ions and the metal-protein
51 244 complexes were analyzed by ESI-Q-TOF. In the absence of Cu, one peak was recorded
52 245 corresponding to the monomeric form of RcnB (Fig. 1B). In the presence of Cu, this peak was
53 246 displaced from a mass corresponding exactly to one atom of Cu (63 Da) (Fig. 1B). No other
54 247 peaks were observed on the whole spectrum indicating that Cu did not modify the oligomeric
55
56
57
58
59
60

1
2
3 248 state of RcnB. This observation was strengthened by a size-exclusion chromatography
4 249 experiment that revealed the same elution volume for the apo and the Cu-bound forms of
5 250 RcnB (data not shown). Taken together, these results indicate that RcnB binds one atom of Cu
6 251 per monomer.

7
8
9 252 Isothermal titration calorimetry was employed in order to determine the dissociation
10 253 constant of the RcnB-Cu complex. The titration of Cu(II) into a solution of apo-RcnB in 10
11 254 mM Pipes buffer pH 7.0 showed significant changes in enthalpy (Fig. 1C). A one-site binding
12 255 model was used to fit the data, yielding a K_D value of 1.8 μM (+/- 0.8) and a stoichiometry of
13 256 Cu to RcnB of 0.81 (+/- 0.01). The experiment was repeated in different buffers (10 mM
14 257 cacodylate, pH 7.0; 10 mM Hepes pH 7.0), using concentrations of RcnB ranging from 50 to
15 258 300 μM , resulting in similar results ($K_D= 1.8 - 6 \mu\text{M}$, $N=0.8-0.9$) (data not shown). Taken
16 259 together, these results show that RcnB binds one atom of Cu per monomer with a micromolar
17 260 affinity.

18 261 ITC was also performed in the same conditions using Ni or Co and no changes in
19 262 enthalpy were observed suggesting that in these cases the K_D is significantly higher than 100
20 263 μM (data not shown).

21 264

22 265 **Cu acts on RcnB stability**

23 266 Native RcnB displayed a far-ultraviolet circular dichroism spectrum with a positive peak at
24 267 230 nm probably due to aromatic residues²⁵ and a negative peak around 210 nm (Fig. 2A). A
25 268 bioinformatic deconvolution of the spectrum of the apo-protein predicted mainly beta sheets
26 269 as secondary structures, about 40 percent of the total protein, whereas the other half was
27 270 randomly folded and helical structures were largely under-represented with circa 5%. RcnB
28 271 shares 71 % identity with YohN of *Klebsiella pneumoniae* whose structure has been solved by
29 272 NMR in the absence of any ligand (PDB :2L1S, Wahab A., Serrano P., Geralt M. and
30 273 Wuthrich K.). The CD data obtained here for RcnB are compatible with this structure which
31 274 contains 15 % helical and 36 % beta sheet secondary structures. When recorded in the
32 275 presence of 1 equivalent of Cu or Ni, the spectra superimposed perfectly indicating that these
33 276 two metals did not induce major secondary structure rearrangements (not shown). The apo-
34 277 RcnB protein was denatured by increasing the temperature to a maximum of 90°C and then
35 278 renatured by decreasing the temperature to 25°C. Spectra before and after thermal
36 279 denaturation of apo-RcnB superimposed indicating that the process was fully reversible (Fig.
37 280 2A). The thermal denaturation was followed after addition of one equivalent of Ni or Cu ions
38 281 (Fig. 2B). In the presence of Ni the denaturation process was similar to the one obtained for

1
2
3 282 the apo-protein adding an evidence of the absence of any interaction between RcnB and these
4 283 ions (Fig. 2B). In contrast, the protein folding was modified when denaturation occurred in
5 284 the presence of Cu ions showing that Cu ions modulate RcnB stability. The T_m value (50 %
6 285 of unfolded form) was 75°C in the presence of Cu whereas it was 86°C for apo-RcnB.
7
8
9
10

11 287 **Cu binding by RcnB is physiological**

12 288 We have shown that RcnB is able to bind Cu *in vitro*. To investigate the hypothesis of
13 289 a physiological incidence of this interaction, as for instance the participation of RcnB to Cu
14 290 resistance in *E. coli*, the resistance against Cu of a strain deleted for the *rcnB* gene was
15 291 studied. After aerobic culture, growth of the wild-type strain was observed only for the most
16 292 concentrated bacterial dilutions when 15 μM Cu was present in the medium (Fig. 3, upper
17 293 panel). The *rcnB* mutant showed exactly the same phenotype indicating that the absence of
18 294 *rcnB* does not increase the cell sensitivity to Cu. In contrast, the metal resistance phenotype
19 295 increased when the *rcnB* mutant was complemented by a plasmid-borne copy of the gene. In
20 296 this case, the growth of the strain was not altered in the presence of metal throughout the
21 297 dilution range, showing enhanced Cu resistance of the bacteria. Under anaerobic growth
22 298 conditions, similar profiles were obtained but the resistance of all the strains was lower (Fig.
23 299 3, lower panel). This increase in Cu toxicity in the absence of oxygen has been previously
24 300 described ²⁶. Therefore, an *rcnB* mutant strain is not more sensitive to Cu but an
25 301 overproduction of the protein can increase significantly the resistance profile.
26
27
28
29
30
31
32
33
34
35

36 302 One explanation for the increased resistance of the complemented strain could be the
37 303 reduced accumulation of free hazardous Cu ions in bacteria. Metal quantification by ICP-OES
38 304 was performed on whole, dried bacteria after growth in LB medium supplemented with 0.5
39 305 mM Cu, a sub-inhibitory concentration. In the presence of Cu, the Cu content in the *rcnB*
40 306 mutant was slightly lower but not significantly different of the level measured in the wild-type
41 307 strain (Table 2). These results are consistent with those of the metal susceptibility test. In
42 308 contrast, complementation of the *rcnB* mutant by *rcnB* hosted on the pUC18 plasmid
43 309 increased twice the cellular Cu content. These results show that RcnB is able to bind Cu *in*
44 310 *vivo* and strongly suggest that the increased Cu resistance of the strain overexpressing RcnB,
45 311 may be linked to the Cu-binding capacity of RcnB which lowers the free Cu content present
46 312 in the periplasm.
47
48
49
50
51
52
53
54
55

56 314 **RcnB is not directly involved in Cu homeostasis**

57
58
59
60

1
2
3 315 To gain insights into the mode of action of RcnB, we investigated the consequences of
4 316 changes in intracellular Cu levels. To achieve this, we studied the connection between *rcnB*
5 317 and the others genetic systems known to be involved in Cu homeostasis in *E. coli*. More
6 318 precisely we studied the periplasmic detoxification systems. Firstly, the consequence of an
7 319 *rcnB* mutation in a *cusF* background was examined. A $\Delta cusF$ mutant was shown to be slightly
8 320 more sensitive to Cu than a wild type strain¹⁷. We have determined if RcnB could have a
9 321 similar role as CusF or substitute for CusF in the absence of this protein. We confirmed that
10 322 the $\Delta cusF$ mutant is more sensitive to Cu than the parental wild type strain (Fig. 4A). When
11 323 assayed, the $\Delta cusF \Delta rcnB$ double mutant showed a similar Cu resistance profile. It indicates
12 324 that RcnB is unrelated to the *cus* system and cannot substitute for CusF as a metallo-
13 325 chaperone working with CusCBA. So, RcnB is a soluble periplasmic Cu-binding protein, like
14 326 CusF, but with a distinct function.

15
16
17
18 327 The other periplasmic Cu detoxification system in *E. coli* is the multi-Cu oxidase
19 328 CueO that is thought to oxidize Cu(I) into its less toxic form Cu(II)²⁶. The MIC of a $\Delta cueO$
20 329 strain was determined in liquid cultures. As previously shown²⁶, the $\Delta cueO$ strain was more
21 330 sensitive to Cu than the wild-type strain (Fig. 4B). The $\Delta rcnB$ mutant displayed a resistance
22 331 pattern similar to the wild-type strain consistent with the assay on Petri dishes (Fig. 3).
23 332 Finally, the $\Delta rcnB \Delta cueO$ double mutant had a growth phenotype similar to the single $\Delta cueO$
24 333 mutant as Cu increased (Fig. 4B). These results confirm that *rcnB* is not involved in Cu
25 334 homeostasis and that *rcnB* is not required by the *cue* system for Cu detoxification. We
26 335 analyzed further the *in vivo* Cu binding capacities of RcnB in a *cueO* mutant. When
27 336 complemented by *rcnB*, borne on a high copy plasmid, the Cu resistance of the $\Delta cueO$ strain
28 337 was restored (Fig. 4C). This can be interpreted, in the light of our previous results (Fig. 3 and
29 338 Table 2), as the consequence of Cu binding by RcnB in the periplasm. Since the expression of
30 339 the *cueO* gene was previously shown to be inducible by silver²⁷ we investigated the behavior
31 340 of the strains in the presence of this metal. We confirmed that the $\Delta cueO$ mutant was slightly
32 341 more sensitive to silver than the wild-type strain (Fig. 4C). However, complementation of the
33 342 $\Delta cueO$ mutant by *rcnB* hosted on the high-copy plasmid pUC18 did not restore the wild-type
34 343 phenotype towards Ag resistance, indicating that RcnB response is specific to Cu.

35
36
37
38
39
40
41
42
43
44
45
46
47
48
49
50
51
52 344 To gain insight into the role of *rcnB*, its expression was followed using RT-PCR.
53 345 When using a primer annealing 162 bp upstream of the ATG of *rcnB* and a primer
54 346 complementary to the end of *rcnB*, transcripts were detected only after growth in the presence
55 347 of Ni or Co (Fig. 4, *rcnB_{ext}*). When primers internal to *rcnB* were used, transcripts were
56
57
58
59
60

1
2
3 348 detected after growth in LB medium or supplemented with Ni or Co or Cu with more
4 349 transcripts detected after growth in the presence of Ni or Co (Fig. 4, *rcnB*_{int}). It has been
5 350 previously shown that *rcnB* is transcribed from the promoter of *rcnA* and that this
6 351 transcription is specifically induced by Ni and Co¹¹. This regulation of expression is observed
7
8 352 with primers external to *rcnB*. When using primers internal to *rcnB*, transcripts are detected in
9 353 all growth conditions and in particular in the absence of the cognate inducers Ni and Co. This
10 354 demonstrates that *rcnB* is constitutively expressed and suggests that a second promoter might
11 355 exist upstream of *rcnB*, the 200 pb *rcnA-rcnB* intergenic region being compatible with this
12 356 hypothesis. In contrast, expression of the *cusF* gene was detected only after growth in LB
13 357 supplemented with Cu (Fig. 4D). As for *cueO*, its expression was detected after growth under
14 358 all the tested conditions, but it was strongly induced by Cu (Fig. 4D). These results show that,
15 359 in contrast to genes related to copper metabolism, *rcnB* is not induced by copper, and dismiss
16 360 *rcnB* as being involved in controlling copper homeostasis in *E. coli*.
17
18 361

362 **Mutant RcnB-M86A deficient in Cu binding is deficient in controlling Ni and Co** 363 **homeostasis**

364 When Cu was added to purified RcnB, the solution turned blue. The metallation of
365 RcnB by Cu was monitored by following the spectral changes between 350 and 850 nm.
366 Addition of increasing amount of Cu lead to the appearance of an absorption band at 610 nm
367 (Fig. 5). The signal increased linearly up to 15 equivalents of Cu, no saturation was observed.
368 Above 15 equivalents, the protein precipitated. In reason of the absence of saturation of RcnB
369 by Cu, the extinction coefficient could not be deduced from the spectra. The metallation of
370 RcnB was carried out in the presence of competitors: EDTA, a strong affinity divalent cations
371 chelator, or glycine, a weaker affinity chelator (K_d of Cu(II) for glycine is *circa* 500 nM at
372 pH 7.5²⁸) and followed by UV-visible spectroscopy. In neither case RcnB was able to
373 compete with the chelators (not shown), confirming that the dissociation constant (K_D) of Cu
374 for RcnB is significantly higher than 500 nM.

375 The extinction of fluorescence of RcnB upon the addition of Cu (Fig. 1A) suggests
376 that at least one of the two tryptophans present in RcnB is close to the Cu-binding site.
377 Alignment of the sequences of homologs of RcnB highlighted the presence of a conserved
378 motif in enterobacteria: H₈₂W₈₃XXM₈₆. Methionine and histidine residues being potent Cu
379 ligands, H82 and M86 mutants were constructed by site directed mutagenesis in which His₈₂
380 or Met₈₆ were substituted with Ala. The mutant proteins were over-expressed and purified
381 using the same protocol as for the wild type protein. Mutant H82A RcnB appeared to be

1
2
3 382 highly unstable, prone to degradation, preventing its purification and further analysis. The
4 383 binding of Cu to the M86A mutant protein was monitored by UV-visible spectroscopy.
5 384 Addition of up to 10 equivalents of Cu did not trigger the appearance of the absorption band
6 385 centered at 610 nm as observed for the wild type protein (Fig. 5 inset). In fact no changes of
7 386 the spectra could be detected when Cu was added, indicating that M86A RcnB had lost the Cu
8 387 center detected in the wild type protein, and in turn that the Cu center giving rise to the
9 388 610nm absorption band involves Cu liganding by M₈₆.

10
11
12
13
14 389 As we have shown previously ¹¹, the biological function of RcnB is to participate in
15 390 the efflux of Ni and Co ions mediated by the efflux pump RcnA. All the data presented here
16 391 show that RcnB is a Cu-binding protein, that it is not involved in maintaining Cu homeostasis.
17 392 It can be hypothesized that the binding of Cu by RcnB is required for its biological function
18 393 i.e. maintaining Ni and Co homeostasis. To address this question, the gene encoding mutant
19 394 M86A RcnB was introduced into an expression vector and its function was determined by
20 395 measuring the susceptibility of the tested strain to Ni or Co toxicity. To ensure stoichiometric
21 396 amounts of RcnR, RcnA and RcnB, we used a plasmid containing *rcnR-rcnAB* in a pUC18
22 397 backbone (pAR123 ⁸). The same plasmid was subjected to site directed mutagenesis to encode
23 398 for an M86A RcnB variant (pMG10). These plasmids were introduced into strain EGE119 a
24 399 $\Delta rcnA\Delta rcnB$ double deletion mutant. As expected the $\Delta rcnAB$ mutant was more sensitive to
25 400 Ni and Co than the WT strain indicating a default in Ni and Co efflux and complementation
26 401 by pAR123 restored the wild type phenotype (Fig. 6A). Most interestingly, when the mutation
27 402 M86A was introduced into *rcnB*, the complementation phenotype was lost, indicating that the
28 403 RcnAB efflux system was no longer functional. Western blot using antibodies directed
29 404 against RcnB was performed to monitor the stability of M86A RcnB. As expected, in crude
30 405 extracts, both the precursor and mature forms of RcnB were detected (Fig. 6B). The mature
31 406 form corresponding to the periplasmic form of RcnB was equally detected in extracts
32 407 expressing the wild-type or the M86A variant of RcnB showing that the mutation did not alter
33 408 the stability of the protein.

34
35
36
37
38
39
40
41
42
43
44
45
46
47
48 409 RcnB shares 71 % identity with YohN of *Klebsiella pneumoniae* whose structure has
49 410 been solved by NMR in the absence of any ligand (PDB :2L1S, Wahab A., Serrano P., Geralt
50 411 M. and Wuthrich K., unpublished) (Supplementary Figure 2). The overall structure is in
51 412 agreement with CD spectra obtained in this study for RcnB of *E. coli*. The surface
52 413 representation shows that the potential Cu coordinating residue M86 is accessible to the
53 414 solvent (Supplementary Fig. 2, B). The modeled structure of YohN was used to examine the
54 415 PDB in order to retrieve structural neighbors using PDBefold ³². No protein structure
55
56
57
58
59
60

1
2
3 416 similarity was detected, emphasizing the fact that the Cu-binding site present in RcnB is
4 417 novel.

5 418

6 419

7 420

Discussion

8 421 The RcnB protein was previously shown to be a periplasmic accessory protein involved in Ni
9 422 and Co efflux in conjunction with the RcnA pump. However it lacks affinity for Ni and Co
10 423 ions ¹¹. In the present work we demonstrate that RcnB is a Cu-binding protein. The first
11 424 evidence came from tryptophan fluorescence quenching experiments where Cu was the only
12 425 tested divalent cation able to quench tryptophan fluorescence (Fig. 1). Cu binding was further
13 426 evidenced by UV-visible spectroscopy (Fig. 5). The binding stoichiometry determined by
14 427 mass spectrometry and ITC led to the conclusion that RcnB binds one Cu per monomer, with
15 428 a dissociation constant in the micromolar range (Fig. 1). This affinity is relevant for a
16 429 biological function, however it is weak when compared to known periplasmic copper-binding
17 430 proteins participating in mechanisms of Cu cell detoxification. For instance *copH* encoded by
18 431 the large plasmid pMOL30 of *Cupriavidus metallidurans* is part of the *cop* cluster involved in
19 432 detoxification of copper. CopH is a periplasmic protein shown to bind Cu(II) on a high
20 433 affinity site with a K_D of 36 nM and on a low affinity site with a K_D of 2.5 μ M ²⁹.

21 434 As the RcnA efflux pump was shown to play a role in Ni or Co but not in Cu resistance ⁸,
22 435 RcnB was not expected to bind copper and the certainty of *in vivo* Cu binding was questioned.
23 436 To address this point, *rcnB* was expressed from a high copy plasmid. In these conditions,
24 437 *rcnB* conferred the cells enhanced Cu resistance combined with increased Cu accumulation in
25 438 cells (Fig. 3 and Table 2). These experiments clearly showed that RcnB binds Cu *in vivo*. All
26 439 together the *in vitro* and *in vivo* experiments demonstrate that RcnB is a new copper protein as
27 440 it shares no homology to previously described proteins.

28 441 *E. coli* possesses two chromosomally encoded periplasmic Cu-proteins, CueO and CusF.
29 442 CueO is a multicopper oxidase able to oxidize Cu(I) in its less toxic form Cu(II) ³⁰. CusF is
30 443 the periplasmic metallochaperone of the RND Cu-efflux system CusCBA ¹⁸. Both CueO and
31 444 CusF are involved in Cu detoxification. While the transcription of *cueO* is induced by copper
32 445 via the cytoplasmic metallo-regulator CueR, the copper induction of the *cusCFBA* operon is
33 446 under the control of the two-components system CusSR able to sense periplasmic copper
34 447 concentration ²⁶. A possible function of RcnB would also be to participate in copper
35 448 detoxification. The CMI of the *rcnB* mutant towards Cu was the same as the wild type strain
36 449 (Fig. 4). Since *E. coli* contains multiple Cu detoxification systems, the *rcnB* mutation can

1
2
3 450 remain silent in reason of compensation by the other systems. However *rcnBcusF* and
4 451 *rcnBcueO* double mutants displayed no enhanced Cu sensitivity compared to *cusF* and *cueO*
5 452 mutants respectively (Fig. 4). Moreover, in contrast to *cueO* or *cusF*, the expression of *rcnB*
6 453 was not induced by Cu. We show here that *rcnB* is expressed on two transcripts: a long
7 454 transcript arising from transcription at the *rcnA* promoter specifically induced by Ni or Co
8 455 (10, 12) and a smaller one expressed in all growth conditions including that without metal.
9 456 Therefore, Cu is not an inducer of the expression of *rcnB* and *rcnB* is likely to be transcribed
10 457 from its own promoter in harmony with the wide 218 bp *rcnA-rcnB* intergenic region.
11 458 Sequence analysis of RcnB homologs among proteobacteria revealed that it can be encoded
12 459 by an orphan gene, which suggests that RcnB-like proteins could also play a role unrelated to
13 460 Ni and Co efflux and resistance. Besides CueR or CusR binding sites were not retrieved in the
14 461 promoter region. Moreover transcriptomic studies of Cu-stressed *E. coli* cells did not identify
15 462 *rcnB* among the Cu-regulated genes³¹. Taken together our results rule out the possibility that
16 463 *rcnB* is part of a Cu detoxification system. Interestingly enough, when expressed on a high
17 464 copy plasmid under the control of the *lac* promoter, *rcnB* complemented a *cueO* deficient
18 465 strain (Fig. 4C). Thus, overproduced RcnB is able to substitute periplasmic CueO, the enzyme
19 466 that detoxifies Cu as it can bind Cu in the same cellular compartment. This complementation
20 467 was not observed for *cus* deficient strains (data not shown).
21 468 At the sequence level, RcnB does not contain any previously described Cu binding site. Still
22 469 RcnB contains 2 methionines, 3 histidines, 11 acidic residues but no cysteine in its mature
23 470 form as potent Cu ligands. It has a potential metal-binding motif H₈₂W₈₃XXM₈₆, well
24 471 conserved among RcnB homologs found in proteobacteria, that we investigated by site-
25 472 directed mutagenesis. While the H82A mutant protein appeared to be unstable when
26 473 overexpressed, purification of the M86A mutant protein was successful. This mutant lost the
27 474 spectroscopic signature of the wild type protein characterized by a broad band centered at 610
28 475 nm upon Cu addition (Fig. 5). It can be concluded that Cu binding by RcnB involves at least
29 476 one methionine residue. RcnB shares 71 % identity with YohN of *Klebsiella pneumoniae*
30 477 whose structure has been solved by NMR in the absence of any ligand (PDB :2L1S, Wahab
31 478 A., Serrano P., Geralt M. and Wuthrich K.). The CD data obtained here for RcnB are
32 479 compatible with this structure. No change of the spectrum was detected on addition of Cu or
33 480 Ni indicating that the global fold of the protein was preserved with metal. Protein Data Bank
34 481 search using the structure of YohN or using models of RcnB based on this latter were
35 482 performed using PDBefold³² and failed to retrieve any structural neighbors.

1
2
3 483 At the physiological level, mutation M86A rendered the RcnAB efflux system ineffective
4 484 with respect to Ni and Co resistance (Fig. 6). This suggests that copper binding by RcnB is
5 485 essential for its function. In light of the CD experiments it can be hypothesized that Cu plays a
6 486 structural role as it was shown to destabilize RcnB leading to precipitation of the protein
7 487 when subjected to thermal denaturation (Fig. 2). One can also suggest that RcnB requires Cu
8 488 to bind Ni or Co as free ions or in complex with prosthetic groups, It has been shown at least
9 489 for Ni that NikA, the periplasmic binding protein of the Ni ABC importer NikABCDE is
10 490 unable to bind Ni directly but requires an organic chelator as a nickelophore. Small organic
11 491 ligands³³ as well as (L-His)₂^{34 35} have been identified as nickelophores. In the case of RcnB,
12 492 Cu could favor such interactions or could favor the binding of Co or Ni ions. Still, Ni binding
13 493 on a Cu-loaded form of RcnB or Cu loading in the presence of Ni were assayed and
14 494 monitored by fluorescence and UV-visible spectroscopy and no differences were observed
15 495 when compared to the metallation assays performed in the presence of Cu only (data not
16 496 shown). Further work aiming at determining the structure of RcnB in interaction with metals
17 497 will help in better understanding its function.
18 498

499 **Acknowledgements**

500 This work was supported by CNRS, INSA Lyon BQR. C.B. and M.G. were supported by a
501 grant from the French Ministry of Research. We thank R. Montserret of IBCP for supervision
502 of the CD and ITC experiments and G. Effantin for technical assistance.
503

504 **References**

- 505 1. S. Okamoto and L. D. Eltis, *Metalloomics*, 2011, **3**, 963-970.
- 506 2. A. M. Sydor and D. B. Zamble, *Metal ions in life sciences*, 2013, **12**, 375-416.
- 507 3. D. Osman and J. S. Cavet, *Adv Appl Microbiol*, 2008, **65**, 217-247.
- 508 4. J. L. Hobman, K. Yamamoto and T. Oshima, *Microbiology monographs*, 2007, D.H.
509 Nies, S. Silver eds : Molecular microbiology of heavy metals, 73-115.
- 510 5. J. Ueda, M. Takai, Y. Shimazu and T. Ozawa, *Arch Biochem Biophys*, 1998, **357**, 231-
511 239.
- 512 6. P. Ray and e. al, *Metalloomics*, 2013.
- 513 7. F. Barras and M. Fontecave, *Metalloomics*, 2011, **3**, 1130-1134.
- 514 8. A. Rodrigue, G. Effantin and M. A. Mandrand-Berthelot, *J Bacteriol*, 2005, **187**,
515 2912-2916.
- 516 9. J. S. Iwig, J. L. Rowe and P. T. Chivers, *Mol Microbiol*, 2006, **62**, 252-262.
- 517 10. D. Blaha, S. Arous, C. Bleriot, C. Dorel, M. A. Mandrand-Berthelot and A. Rodrigue,
518 *Biochimie*, 2011, **93**, 434-439.
- 519 11. C. Bleriot, G. Effantin, F. Lagarde, M. A. Mandrand-Berthelot and A. Rodrigue, *J*
520 *Bacteriol*, 2011, **193**, 3785-3793.
- 521 12. L. Decaria, I. Bertini and R. J. P. Williams, *Metalloomics*, 2011, **3**, 56-60.

- 1
2
3 522 13. A. Changela, K. Chen, Y. Xue, J. Holschen, C. E. Outten, T. V. O'Halloran and A.
4 523 Mondragon, *Science*, 2003, **301**, 1383-1387.
5 524 14. C. Rensing and G. Grass, *FEMS Microbiol Rev*, 2003, **27**, 197-213.
6 525 15. G. Grass and C. Rensing, *Biochem Biophys Res Commun*, 2001, **286**, 902-908.
7 526 16. S. K. Singh, G. Grass, C. Rensing and W. R. Montfort, *J Bacteriol*, 2004, **186**, 7815-
8 527 7817.
9 528 17. S. Franke, G. Grass, C. Rensing and D. H. Nies, *J Bacteriol*, 2003, **185**, 3804-3812.
10 529 18. E.-H. Kim, D. H. Nies, M. M. McEvoy and C. Rensing, *J. Bacteriol.*, 2011, **193**,
11 530 2381-2387.
12 531 19. G. Grass and C. Rensing, *J Bacteriol*, 2001, **183**, 2145-2147.
13 532 20. T. Baba, T. Ara, M. Hasegawa, Y. Takai, Y. Okumura, M. Baba, K. A. Datsenko, M.
14 533 Tomita, B. L. Wanner and H. Mori, *Mol Syst Biol*, 2006, **2**.
15 534 21. J. H. Miller, *Cold Spring Harbor, N.Y.: Cold Spring Harbor Laboratory*, 1992.
16 535 22. A. J. Link, D. Phillips and G. M. Church, *J Bacteriol*, 1997, **179**, 6228-6237.
17 536 23. J. Y. Jeong, H. S. Yim, J. Y. Ryu, H. S. Lee, J. H. Lee, D. S. Seen and S. G. Kang,
18 537 *Appl Environ Microbiol*, 2012, **78**, 5440-5443.
19 538 24. L. Whitmore and B. A. Wallace, *Nucleic Acids Res*, 2004, **32**, W668-673.
20 539 25. R. W. Woody, *Eur Biophys J*, 1994, **23**, 253-262.
21 540 26. F. W. Outten, D. L. Huffman, J. A. Hale and T. V. O'Halloran, *J Biol Chem*, 2001,
22 541 **276**, 30670-30677.
23 542 27. J. V. Stoyanov and N. L. Brown, *J Biol Chem*, 2003, **278**, 1407-1410.
24 543 28. R. M. C. Dawson, D. C. Elliot, W. H. Elliot and K. M. Jones, *Clarendon press*,
25 544 *Oxford*, 1986, **3rd edition**.
26 545 29. V. Sendra, S. Gambarelli, B. Bersch and J. Coves, *J Inorg Biochem*, 2009, **103**, 1721-
27 546 1728.
28 547 30. K. Y. Djoko, L. X. Chong, A. G. Wedd and Z. Xiao, *J Am Chem Soc*, 2010, **132**,
29 548 2005-2015.
30 549 31. K. Yamamoto and A. Ishihama, *Mol Microbiol*, 2005, **56**, 215-227.
31 550 32. E. Krissinel and K. Henrick, *Acta Crystallogr D Biol Crystallogr* 2004, **60**, 2256-
32 551 2268.
33 552 33. M. V. Cherrier, C. Cavazza, C. Bochot, D. Lemaire and J. C. Fontecilla-Camps,
34 553 *Biochemistry*, 2008, **47**, 9937-9943.
35 554 34. P. T. Chivers, E. L. Benanti, V. Heil-Chapdelaine, J. S. Iwig and J. L. Rowe,
36 555 *Metallomics*, 2012, **4**, 1043-1050.
37 556 35. H. Lebrette, M. Iannello, J. C. Fontecilla-Camps and C. Cavazza, *J Inorg Biochem*,
38 557 2013, **121**, 16-18.
39 558 36. F. W. Studier, A. H. Rosenberg, J. J. Dunn and J. W. Dubendorff, *Methods Enzymol*,
40 559 1990, **185**, 60-89.
41 560 37. C. Yanisch-Perron, J. Vieira and J. Messing, *Gene*, 1985, **33**, 103-119.
42 561
43 562
44 563
45 564
46 565
47 566
48 567
49 568

Figure legends

Figure 1

RcnB is a Cu binding protein. (A) Fluorescence quenching after the addition of increasing amounts of CuSO₄. Protein was dissolved in 100 mM Bis-Tris propane buffer (pH 6.0) to a final concentration of 5 μM. At each step, a ten-fold excess of metal ions solution was titrated into the protein solution. Fluorescence intensity was monitored between 300 and 400 nm after

1
2
3 569 an excitation at $\lambda = 280$ nm. Intensity is expressed in arbitrary units. (B) Mass spectra of
4 570 RcnB (5 μ M) reconstituted with or without a ten-fold excess of Cu^{2+} ions in 20 mM
5 571 ammonium acetate buffer (pH 7.0). The mass spectrum of apo-RcnB (upper panel) or after the
6 572 addition of 10 equivalents of Cu^{2+} (panel below) is shown. (C) Isothermal titration calorimetry
7 573 of RcnB. Cu(II)SO_4 (1.5 mM) titrated into apo-RcnB (150 μ M) in 10 mM Pipes buffer (pH 7)
8 574 at 30°C. Top, raw data. Bottom, plot of integrated heats versus Cu/RcnB ratio. The solid line
9 575 represents the best fit for a one-site binding model.
10
11
12
13
14
15

576

577 **Figure 2**

16 578 **Cu acts on RcnB stability.** (A) CD spectra of RcnB (25 μ M) in 50 mM mM sodium
17 579 phosphate buffer (pH 7.0) at 25°C before (solid line) or after (dashed line) thermal
18 580 denaturation at 90°C. **B.** CD-monitored thermal denaturation of apo-RcnB (solid line), RcnB
19 581 in the presence of Ni (dotted and dashed line) or RcnB in the presence of Cu (dashed line).
20 582 The value of CD at 220 nm is used to estimate the fraction of unfolded RcnB.
21
22
23
24
25

583

26 584 **Figure 3**

27
28 585 **Cu binding by RcnB is physiological.** The wild-type strain (W3110), the Δ *rcnB* isogenic
29 586 mutant (WRCB1), WRCB1 pUC18, and WRCB1 pUCRCB (*rcnB* in pUC18) were grown in
30 587 LB medium to mid-log phase. A 10-fold serial dilution of the cultures was performed, and 5
31 588 μ l was spotted on M63 minimal medium supplemented with 0.4% glucose (G), 0.4% glucose
32 589 plus 10 or 15 μ M CuSO_4 and grown aerobically (top) or anaerobically (bottom) at 37°C in
33 590 Petri dishes. Spots corresponding to 10^7 (rightmost column) to 10^4 (leftmost column) bacteria
34 591 are shown.
35
36
37
38
39
40

592

41 593 **Figure 4**

42 594 **RcnB is not directly involved in Cu homeostasis.** (A). The wild-type strain (W3110),
43 595 Δ *rcnB*, Δ *cusF* and Δ *rcnB* Δ *cusF* isogenic mutants were grown in LB medium to mid-log
44 596 phase. A 10-fold serial dilution of the cultures was performed, and 5 μ l was spotted on M63
45 597 minimal medium supplemented with 0.4% glucose (G), 0.4% glucose plus 2 μ M CuSO_4 and
46 598 grown anaerobically on Petri dishes. Spots corresponding to 10^7 (rightmost column) to 10^4
47 599 (leftmost column) bacteria are shown. (B) The wild-type strain (W3110), Δ *rcnB*, Δ *cueO* and
48 600 Δ *rcnB* Δ *cueO* isogenic mutants were grown in M63 minimal medium supplemented with
49 601 0.4% glucose (G) plus increasing amounts of CuSO_4 . $\text{OD}_{600\text{nm}}$ was recorded after 16 hours
50 602 aerobic incubation at 37°C. (C) The wild-type strain (W3110), Δ *cueO* isogenic mutant
51
52
53
54
55
56
57
58
59
60

1
2
3 603 complemented or not with pUCRCB were grown as in (A) and 5 μ l was spotted on M63
4 604 minimal medium supplemented with 0.4% glucose (G), or 0.4% glucose plus 10 μ M CuSO₄
5 605 or 1 μ M AgSO₄ and grown aerobically on Petri dishes. Spots corresponding to 10⁷ (rightmost
6 606 column) to 10⁴ (leftmost column) bacteria are shown. (D). Total RNA was extracted from WT
7
8 607 bacteria grown in LB medium alone or supplemented with non-inhibitory amounts of NiSO₄,
9 608 CoCl₂ or CuSO₄. RNA were PCR amplified without (RTase -) or with (RTase +) a reverse
10 609 transcription step. The amplification was performed by using specific primers for *rcnB*, *cusF*
11 610 or *cueO* genes. A representative agarose gel is shown.
12
13
14
15
16
17

18 612 **Figure 5**

19 613 **Methionine 86 is involved in Cu binding.** (A). UV-visible Cu titration of 130 μ M RcnB or
20 614 80 μ M RcnBM86A (inset) in 50 mM Tris-HCl buffer (pH 7.0) with CuSO₄ at 25°C. The
21 615 differential spectra corresponding to the subtraction of the spectrum of the apo protein are
22 616 shown.
23
24
25
26
27

28 618 **Figure 6**

29 619 **Methionine 86 mutants are deficient in controlling Ni and Co homeostasis** (A) The wild-
30 620 type strain W3110 (closed symbols) and EGE119 Δ *rcnA* Δ *rcnB* isogenic mutant (open
31 621 symbols) complemented with pUC18 (vector) or pAR123 (*rcnR-rcnAB*) or pMG10 (as
32 622 pAR123 but M86A RcnB) were grown in LB medium to mid-log phase. A 10-fold serial
33 623 dilution of the cultures was performed, and 5 μ l was spotted on M63 minimal medium
34 624 supplemented with 0.4% glucose (G), 0.4% glucose plus 40 μ M NiSO₄ or 0.4% glucose plus
35 625 5 μ M CoCl₂ and grown aerobically on Petri dishes. Spots corresponding to 10² (rightmost
36 626 column) to 10⁷ (leftmost column) bacteria are shown. (B) Western blot against RcnB. Lane 1 :
37 627 BL21/pETRCB, lane 2 : BL21/pET30, lane 3: BL21/pETRBM. RcnB-p : precursor form,
38 628 RcnB-m : mature form.
39
40
41
42
43
44
45
46
47
48
49
50
51
52
53
54
55
56
57
58
59
60

631 **Table 1 : Strains and plasmids used in this study**

632

Strains or plasmids	Genotype or description	Source, reference
strains		
BW25113	<i>lacIq rrnBT14 _lacZ</i> WJ16 <i>hsdR514 _araBAD</i> AH33 <i>_rhaBAD</i> LD78	20
JW0119	BW25113, Δ <i>cueO::kanR</i>	20
JW0562	BW25113, Δ <i>cusF::kanR</i>	20
W3110	Wild type	Laboratory stock
WRCB1	W3110, Δ <i>rcnB::cm</i>	11
WCUF1	W3110, Δ <i>cusF::kanR</i>	This study
WCUE1	W3110, Δ <i>cueO::kanR</i>	This study
WRBC1	WRCB1, Δ <i>cueO::kanR</i>	This study
WRBF1	WRCB1, Δ <i>cusF::kanR</i>	This study
EGE119	W3110 Δ <i>rcnA</i> Δ <i>rcnB</i>	This study
BL21	F- <i>ompT gal [dcm] [lon] hsdSB</i> (rB- mB-) (DE3)	36
plasmids		
pKO3	<i>repA</i> (ts) Cm ^R M13ori <i>sacB</i>	22
pEGL16	PCR fragment Δ <i>rcnAB</i> in pKO3	This study
pET30	Overexpression vector	Novagen
pETRCB	pET30 containing <i>rcnB</i> coding sequence	11
pETRBM	As pETRCB with a point mutation in <i>rcnB</i> leading to M86A -RcnB	This study
pUC18	expression vector, Amp ^R	37
pAR123	<i>rcnR-rcnAB</i> in pUC18	8
pMG10	As pAR123 with point mutations in <i>rcnB</i> leading to M86A -RcnB	This study
pUCRCB	pUC18 containing <i>rcnB</i> coding sequence	11

633

634

635

636 **Table 2 Cu content in bacteria**

Strain	WT	$\Delta rcnB$	$\Delta rcnB/rcnB$
Cu ($\mu\text{g/g}$)	75 ± 6	67 ± 1	144 ± 5

637

638 The wild-type strain (W3110), the $\Delta rcnB$ isogenic mutant (WRCB1), and the $\Delta rcnB$ mutant
639 complemented by *rcnB* (WRCB1/pUCRCB) were grown in LB medium supplemented with
640 500 μM CuSO_4 . Values ($\mu\text{g/g}$ bacterial dry weight) are the means of at least three
641 independent ICP-OES measurements performed on independent cultures.

642

643

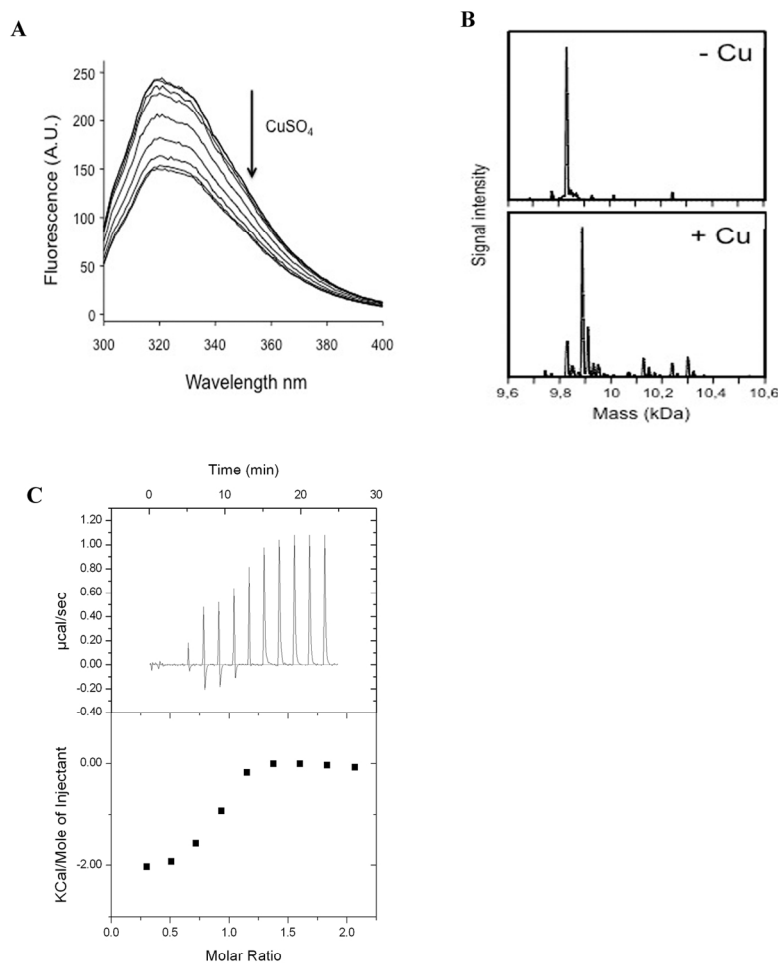


Figure 1

RcnB is a Cu binding protein. (A) Fluorescence quenching after the addition of increasing amounts of CuSO₄. Protein was dissolved in 100 mM Bis-Tris propane buffer (pH 6.0) to a final concentration of 5 µM. At each step, a ten-fold excess of metal ions solution was titrated into the protein solution. Fluorescence intensity was monitored between 300 and 400 nm after an excitation at $\lambda = 280$ nm. Intensity is expressed in arbitrary units. (B) Mass spectra of RcnB (5 µM) reconstituted with or without a ten-fold excess of Cu²⁺ ions in 20 mM ammonium acetate buffer (pH 7.0). The mass spectrum of apo-RcnB (upper panel) or after the addition of 10 equivalents of Cu²⁺ (panel below) is shown. (C) Isothermal titration calorimetry of RcnB. Cu(II)SO₄ (1.5 mM) titrated into apo-RcnB (150 µM) in 10 mM Pipes buffer (pH 7) at 30°C. Top, raw data. Bottom, plot of integrated heats versus Cu/RcnB ratio. The solid line represents the best fit for a one-site binding model.

209x297mm (180 x 180 DPI)

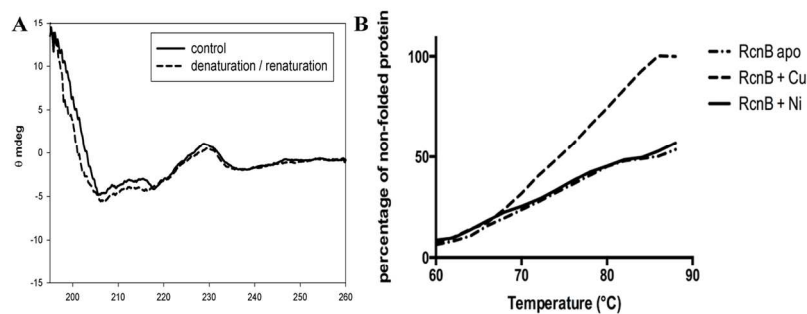


Figure 2

Cu acts on RcnB stability. (A) CD spectra of RcnB (25 μM) in 50 mM sodium phosphate buffer (pH 7.0) at 25°C before (solid line) or after (dashed line) thermal denaturation at 90°C. B. CD-monitored thermal denaturation of apo-RcnB (solid line), RcnB in the presence of Ni (dotted and dashed line) or RcnB in the presence of Cu (dashed line). The value of CD at 220 nm is used to estimate the fraction of unfolded RcnB. 209x297mm (180 x 180 DPI)

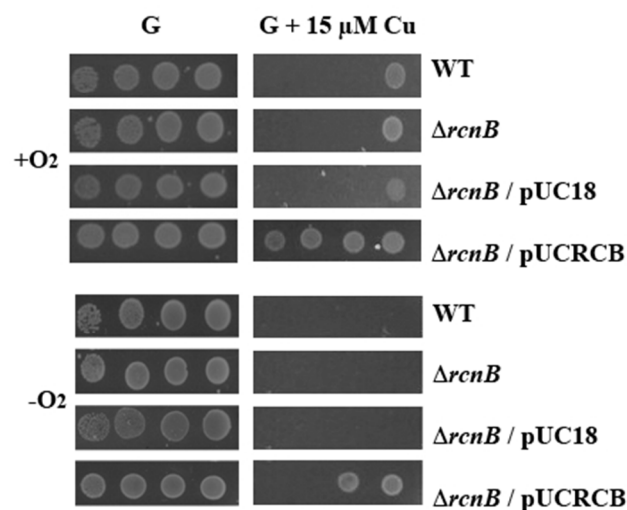


Figure 3

Cu binding by RcnB is physiological. The wild-type strain (W3110), the ΔrcnB isogenic mutant (WRCB1), WRCB1 pUC18, and WRCB1 pUCRCB (rcnB in pUC18) were grown in LB medium to mid-log phase. A 10-fold serial dilution of the cultures was performed, and 5 μl was spotted on M63 minimal medium supplemented with 0.4% glucose (G), 0.4% glucose plus 10 or 15 μM CuSO₄ and grown aerobically (top) or anaerobically (bottom) at 37°C in Petri dishes. Spots corresponding to 10⁷ (rightmost column) to 10⁴ (leftmost column) bacteria are shown.

209x297mm (72 x 72 DPI)

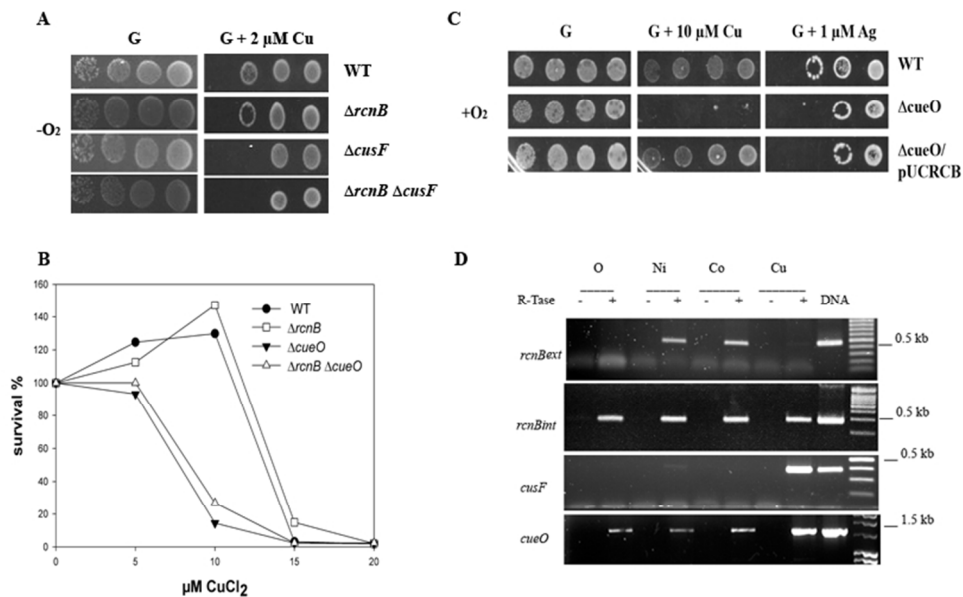


Figure 4

RcnB is not directly involved in Cu homeostasis. (A). The wild-type strain (W3110), $\Delta rcnB$, $\Delta cusF$ and $\Delta rcnB \Delta cusF$ isogenic mutants were grown in LB medium to mid-log phase. A 10-fold serial dilution of the cultures was performed, and 5 μl was spotted on M63 minimal medium supplemented with 0.4% glucose (G), 0.4% glucose plus 2 μM CuSO_4 and grown anaerobically on Petri dishes. Spots corresponding to 107 (rightmost column) to 104 (leftmost column) bacteria are shown. (B) The wild-type strain (W3110), $\Delta rcnB$, $\Delta cueO$ and $\Delta rcnB \Delta cueO$ isogenic mutants were grown in M63 minimal medium supplemented with 0.4% glucose (G) plus increasing amounts of CuSO_4 . OD600nm was recorded after 16 hours aerobic incubation at 37°C. (C) The wild-type strain (W3110), $\Delta cueO$ isogenic mutant complemented or not with pUCRCB were grown as in (A) and 5 μl was spotted on M63 minimal medium supplemented with 0.4% glucose (G), or 0.4% glucose plus 10 μM CuSO_4 or 1 μM AgSO_4 and grown aerobically on Petri dishes. Spots corresponding to 107 (rightmost column) to 104 (leftmost column) bacteria are shown. (D). Total RNA was extracted from WT bacteria grown in LB medium alone or supplemented with non-inhibitory amounts of NiSO_4 , CoCl_2 or CuSO_4 . RNA were PCR amplified without (RTase -) or with (RTase +) a reverse transcription step. The amplification was performed by using specific primers for *rcnB*, *cusF* or *cueO* genes. A representative agarose gel is shown.

297x209mm (72 x 72 DPI)

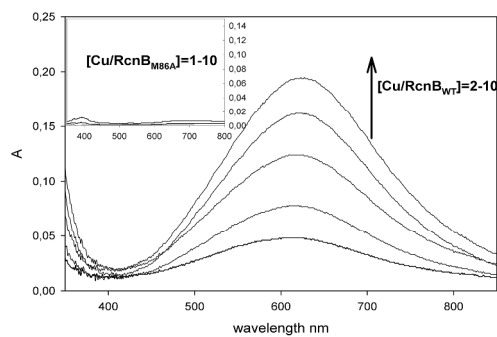


Figure 5

Methionine 86 is involved in Cu binding. (A). UV-visible Cu titration of 130 μ M RcnB or 80 μ M RcnBM86A (inset) in 50 mM Tris-HCl buffer (pH 7.0) with CuSO₄ at 25°C. The differential spectra corresponding to the subtraction of the spectrum of the apo protein are shown.
289x420mm (300 x 300 DPI)

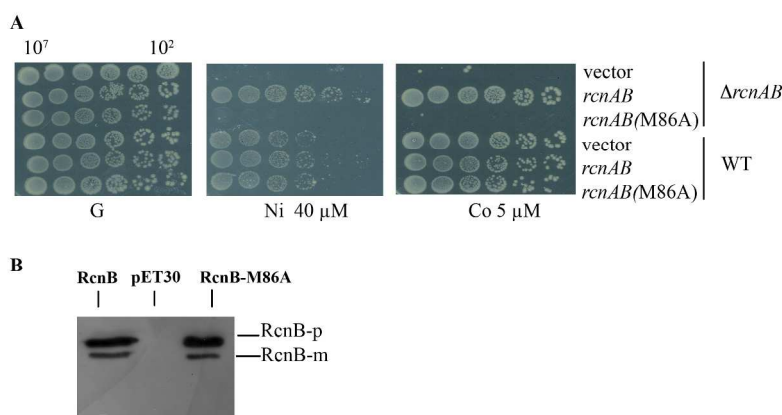


Figure 6

Methionine 86 mutants are deficient in controlling Ni and Co homeostasis (A) The wild-type strain W3110 (closed symbols) and EGE119 $\Delta rcnA\Delta rcnB$ isogenic mutant (open symbols) complemented with pUC18 (vector) or pAR123 (*rcnR-rcnAB*) or pMG10 (as pAR123 but M86A RcnB) were grown in LB medium to mid-log phase. A 10-fold serial dilution of the cultures was performed, and 5 μ l was spotted on M63 minimal medium supplemented with 0.4% glucose (G), 0.4% glucose plus 40 μ M NiSO₄ or 0.4% glucose plus 5 μ M CoCl₂ and grown aerobically on Petri dishes. Spots corresponding to 10² (rightmost column) to 10⁷ (leftmost column) bacteria are shown. (B) Western blot against RcnB. Lane 1 : BL21/pETRCB, lane 2 : BL21/pET30, lane 3: BL21/pETRBM. RcnB-p : precursor form, RcnB-m : mature form.

209x297mm (300 x 300 DPI)